


EFFECT OF MODIFYING THE CLINOPTILOLITE-CONTAINING ROCKS OF TRANSCARPATHIA ON THEIR POROUS CHARACTERISTICS AND CATALYTIC PROPERTIES IN THE CONVERSION OF C₆-HYDROCARBONS

Yuliya Voloshyna¹, , Olexandra Pertko¹, Volodymyr Povazhnyi¹,
Lyubov Patrylak¹, Angela Yakovenko¹

<https://doi.org/10.23939/chcht17.02.373>

Abstract. The efficiency of modifying the Ukrainian clinoptilolite-containing rocks to improve their adsorption and catalytic properties was evaluated based on the data of XRD, IR spectroscopy, low-temperature N₂ adsorption, and testing in the micropulse catalytic transformation of C₆-hydrocarbons. The effect of such modification on the distribution of reaction products was established.

Keywords: zeolite-containing rock, bifunctional catalyst, modification, C₆-hydrocarbons, cracking, hydroisomerization.

1. Introduction

The regularity of the crystal structure of zeolites in combination with the narrow distribution of micropores by size is the determining factor in the form-selective effect of zeolites. However, the downside is the low rate of diffusion of molecules of adsorbates and reagents to active sites (up to their complete inaccessibility in ultramicropores), as well as the slow desorption of reaction products after catalytic transformation. Diffusion hindrances significantly reduce the efficiency of the process and reduce the lifetime of catalysts.¹ As a result, the exclusively microporous nature of zeolites significantly narrows the scope of their application. The diffusion characteristics of the samples can be improved by developing secondary mesoporosity through a post-synthetic modification, which will improve the catalytic properties of zeolite microporous objects.


The combination of micro- and mesoporosity within a single nanostructured material is a promising line of research. Many modern works are devoted to the creation of micro-mesoporous materials and the study of their

use in fine organic synthesis, pharmacy, *etc.*^{2–6} These materials are characterized by increased accessibility of a sorption space and active sites for reagent molecules. As a result, catalytic activity and productivity are increased in reactions that on traditional zeolites proceed with significant steric or diffusion limitations or do not occur at all.

The development of simple and accessible methods for the preparation of zeolite catalysts with a developed porous system is a task of current importance since up to 40% of catalysts in the chemical industry are obtained on the basis of zeolites. A separate significant point is to clarify the prospects to attract Ukrainian raw materials, in particular natural zeolites of Transcarpathia, with the creation of secondary porosity in them at meso- and macrolevels in addition to traditional zeolite microporosity.

According to the literature,^{7–9} one of the most effective catalysts for the isomerization of linear hexane, an industrially important reaction used to increase the octane number of the pentane-hexane fraction of oil, is mordenite. The prospect of using natural zeolites of Transcarpathia with predominantly mordenite components for these purposes was investigated.^{10–14} However, Transcarpathian deposits of zeolite rocks often contain, in a tight genetic mixture with mordenite or separately, clinoptilolite with close to mordenite Si/Al ratio, and therefore, similar acidic characteristics of these natural zeolites can be expected. Clinoptilolite is much less studied as a catalyst for the isomerization of alkanes, however, there are works indicating the effectiveness of natural clinoptilolite of various origins in other catalytic reactions: isomerization of *n*-butene,¹⁵ α -pinene,^{16,17} and limonene,¹⁸ dehydration of methanol,¹⁹ liquid phase hydrogenation of citral.²⁰

To achieve optimal²¹ for isomerization acid site strength, the zeolite rock must be subjected to dealumination, which can serve the dual function of increasing the silicate modulus and developing mesoporosity as an effective way to increase the accessibility of acid sites for reagent molecules due to the formation of structural defects.

¹ V. P. Kukhar Institute of Bioorganic Chemistry and Petrochemistry of National Academy of Sciences of Ukraine
1 Acad. Kukharia St., Kyiv, 02094, Ukraine
 yule.v444@gmail.com

© Voloshyna Yu., Pertko O., Povazhnyi V., Patrylak L., Yakovenko A., 2023

The purpose of the work is the synthesis of zeolite catalysts by acid and alkaline modification of clinoptilolite-containing rocks of Ukrainian deposits and the evaluation of their activity in the conversion of *n*-hexane and 2-methylpentane.

2. Experimental

2.1. Synthesis of Catalysts

Catalysts were synthesized on the basis of two zeolite rocks of Transcarpathia: clinoptilolite rock #1 (Sokyrnytsia village, the content of clinoptilolite is about 80 wt%, the total SiO₂/Al₂O₃ ratio 9.2, the molar composition of the rock (mmol/g): Na₂O – 0.40, K₂O – 0.32, CaO – 0.37, MgO – 0.21, Al₂O₃ – 1.28, SiO₂ – 11.9) and clinoptilolite-mordenite rock #2 (Lypcha village, the content of clinoptilolite and mordenite is 49 and 49 wt. %, the total SiO₂/Al₂O₃ ratio 9.0, the molar composition of the rock (mmol/g): Na₂O – 0.11, K₂O – 0.25, CaO – 0.57, Al₂O₃ – 1.20, SiO₂ – 10.81, H₂O – 6.8). Rocks were crushed to a fraction of 0.5–1 mm.

For the synthesis of the hydrogen form H#1 and H#2 of the rocks, firstly their ammonium form was obtained by ion exchange of cations of the rocks for ammonium ions from a 3 mol/L NH₄NO₃ solution (360 K, 3 h, the ratio of solid phase to liquid (S : L) is 1 : 5). The degree of exchange was controlled by the formaldehyde titration method.²² It made up 94 ± 5 %. The obtained NH₄-form of the rocks was converted into the hydrogen

form by calcination in a muffle furnace at 873 K for 3 hours. In a separate case, the hydrogen form was obtained by treating the sample with a solution of 1.5 mol/L HCl.

Alkaline treatment (360 K, S : L = 1 : 5, 1 h) was carried out using 0.2 mol/L sodium hydroxide solution, and acid treatment (360 K, S : L = 1 : 5, 2 h) was carried out using solutions of hydrochloric acid of various concentrations in the range of 0.5–5 mol/L (Table 1).

Metal component (Ni) was introduced into the catalyst samples by the method of incipient wetness impregnation with an aqueous solution of nickel nitrate hexahydrate Ni(NO₃)₂·6H₂O and reduced in a flow of hydrogen (50 cm³/min) at 653 K for 6 hours.

2.2. Methods

Diffraction patterns of the samples were recorded on a MiniFlex600 diffractometer (Rigaku) in CuK α radiation (0.154178 nm) in the 2 θ angle range of 2–80 degrees with a step of 0.02 degrees and a rotation speed of 5 degree/min. The acceleration voltage was 40 kV, and the anode current was 15 mA. The phase analysis was performed according to the Database of Zeolite Structures.²³

IR spectra of the catalysts in the field of framework vibrations were recorded on the IRAffiniti-1s Fourier spectrometer (Shimadzu, Japan) with a single-reflection ATR accessory Specac Quest GS 10801-B in the region of 400–4000 cm⁻¹. A sample was applied to the surface of the diamond prism of the ATR accessory, and the spectrum was recorded. Spectra were taken relative to air.

Table 1. Modification of catalysts based on natural zeolites of Transcarpathia

An initial form of the rock	Catalyst	Peculiarity of synthesis		Crystallinity ^c , %
		Modifying solution	Concentration, mol/L	
#1	H(#1-B) ^a	NaOH	0.2	29
	#1-A0.5	HCl	0.5	63
	#1-A1	HCl	1	55
	#1-A1.5	HCl	1.5	55
H#1	H#1-A0.5	HCl	0.5	54
	H#1-A1	HCl	1	70
	H#1-A1.5	HCl	1.5	66
#2	H(#2-B) ^b	NaOH	0.2	86
	#2-A1	HCl	1	76
	#2-A5	HCl	5	56
H#2	H#2-A5	HCl	5	62

^a The modification was applied to the native form of the rock, followed by the conversion to the NH₄-form using ammonium nitrate and calcination to obtain the hydrogen form.

^b The modification was applied to the native form of the rock, followed by the conversion to the hydrogen form using hydrochloric acid.

^c Calculated from XRD patterns for the rock #1-based catalysts, and from the IR spectra for the rock #2-based catalysts.

Isotherms of low-temperature (77 K) nitrogen ad(desorption) were measured on a Quantachrome® NOVA 1200e automatic sorbometer after evacuating the samples in situ at a temperature of 568 K for 10 h. NovaWin™ software was used to calculate the parameters of a porous structure of the catalysts. The specific surface area S^{BET} was calculated using the multipoint BET method; the specific surface area not considering micropores S^t and the volume of micropores V_{micro} – by the t -method, the specific surface area of micropores – by the formula $S_{micro} = S^{BET} - S^t$; total pore volume V – by the volume of adsorbed nitrogen at $p/p_0 > 0.99$. The volume of mesopores V_{meso} was calculated according to the formula $V_{meso} = V - V_{micro}$, considering the share of macropores to be insignificant. Pore size distribution was determined using density functional theory (DFT); average pore size R – from the assumption of their cylindrical shape according to the formula $R = 2V/S^{BET}$.

Hydroisomerization of C_6 -hydrocarbons was studied using a setup with a microreactor mounted in the chromatographic line of a TSVET 104 chromatograph. The catalyst with a mass of 0.1 g was activated in a hydrogen flow (flow rate – 20 cm³/min) at 653 K for 1 h before supplying it with hydrocarbon in micropulses of 1.0 μL. The reaction products were trapped at a temperature of 77 K and transferred by a thermal shock to a copper capillary column (length 50 m, inner diameter 0.20 mm, stationary phase Squalane) for separation. The products were analyzed in a hydrogen flow of 50 cm³/min using a flame ionization detector, recording its signal using the Multispectr 1 chromatographic attachment. The flow rate of hydrogen and air through the detector was 30 and 300 cm³/min, respectively, the temperature in the column thermostat made up 323 K.

The test procedure described above was repeated in increments of 25 degrees, starting at 473 K and ending when only cracking products – C_1 – C_5 hydrocarbons – were recorded in the conversion products. As a rule, it was a temperature of 573 K.

The conversion X (wt. %) and selectivity for a j -product S_j (%) were calculated according to the formulas:

$$X = 100 - Y_{C_6},$$

$$S_j = \frac{Y_j}{X},$$

where Y_{C_6} is the yield of unreacted reagent (wt. %), Y_j is the yield of j -product.

The yield of hexane isomers Y_{iC_6} was calculated as the sum of the yields of 2-methylpentane (2-MP), 3-methylpentane (3-MP), and dimethylbutanes (DMB) for the case of the n -hexane conversion, and as the sum of the yields of 3-MP, DMB, and n -hexane for the case of the 2-MP conversion.

3. Results and Discussion

3.1. Characterization of the Samples

The effect of alkaline and acid treatments on the crystallinity of samples of rock #1 was evaluated using XRD. Samples for research were taken before the introduction of the metal component. The degree of crystallinity γ of modified samples (Table 1) was estimated from the relative intensity of the analytical diffraction maximum for clinoptilolite ($d=0,297$ nm). The crystallinity of the original rock was taken as 100%.

The X-ray diffraction patterns of the catalysts based on rock #1 (Fig. 1) contain all the characteristic peaks of clinoptilolite,²³ as well as intense lines of quartz.²⁴ Alkaline treatment (sample H(#1-B)) led to a noticeable decrease in the intensity of clinoptilolite lines, which indicates significant destruction of its crystal structure ($\gamma \sim 30\%$). But in this case, it should also be considered that alkaline treatment usually leads to a decrease in the particle size of the catalysts, which could worsen the X-ray diffraction pattern. Unlike alkaline treatment, the acid treatment had a less significant destructive effect on the crystalline structure. The crystalline structure of the cationic form of the rock begins to be visibly destroyed when the concentration of the modifying acid solution reaches 1 mol/L ($\gamma \sim 55\%$). This is indicated also by the comparison of the intensities of quartz and clinoptilolite lines at 20.9 and 22.5 2θ , respectively. At the same time, the hydrogen form of the rock is more stable, and for the samples modified with 1 mol/L acid ($\gamma \sim 70\%$) and 1.5 mol/L acid ($\gamma \sim 66\%$), the ratio of intensities of these lines is still preserved.

Unlike rock #1, rock #2 contains near 49 % of mordenite. The preservation of the crystalline structure of the mordenite component in rock #2 after alkaline and acid modification was monitored by IR spectroscopy. Fig. 2 shows the IR spectra of the rock #2 samples without the metal component in the region of framework vibration. The reference of the band was made according to the works.^{25,26}

In the IR spectra of mordenite, sensitive to the crystallinity degree is the ratio $R_{560/440}$ of optical densities of absorption bands (a.b.) at 560 and 440 cm⁻¹ assigned to the vibrations of the double 5-membered ring and O–T–O bending vibrations, respectively.²⁶ In the spectrum of the native rock (sample #2), two peaks are observed in the region of 500–600 cm⁻¹ at 520 and 600 cm⁻¹ instead of one a.b. at 560 cm⁻¹. This may be due to the presence of the clinoptilolite component of the rock, but the merging of these bands in the spectrum of decationated sample H#2 indicates that the divergence is rather caused by the diversity of the cationic composition of the native form of the rock. These two a.b. were treated in total. An a.b. at

440 cm^{-1} in the spectra in Fig. 2 takes up a position near 425 cm^{-1} . Comparison of $R_{560/425}$ in the spectra of the modified samples with that for the native rock, similar to that described earlier,²⁷ showed that the γ crystallinity of the mordenite component of the modified catalysts is generally retained (Table 1).

The high-frequency shift of a strong a.b. at 1015 cm^{-1} referred to the asymmetric stretching vibrations of T–O bonds of tetrahedra confirms the framework dealumination of the modified samples. Besides, in the spectrum of the alkali-modified sample H(#2-B) a decrease in the intensity of this band can be observed. We believe that this indicates at least some Al atoms, especially those

belonging to the clinoptilolite component, leave their tetrahedral positions. Such a destruction of the framework tetrahedra is responsible for the somewhat overestimated, in our opinion, values of $R_{560/425}$ and γ for this sample (Table 1). The latter is indirectly confirmed by the results of the X-ray diffraction study of the alkali-treated sample of completely clinoptilolite rock #1. Amorphization, in a varying degree, of the sample H(#2-B) as well as other modified samples is supported by the appearance in their spectra of an a.b. at 935 cm^{-1} , which is often attributed to various types of structural defects. However, the main bands characteristic of zeolite structure are still present in the spectra.

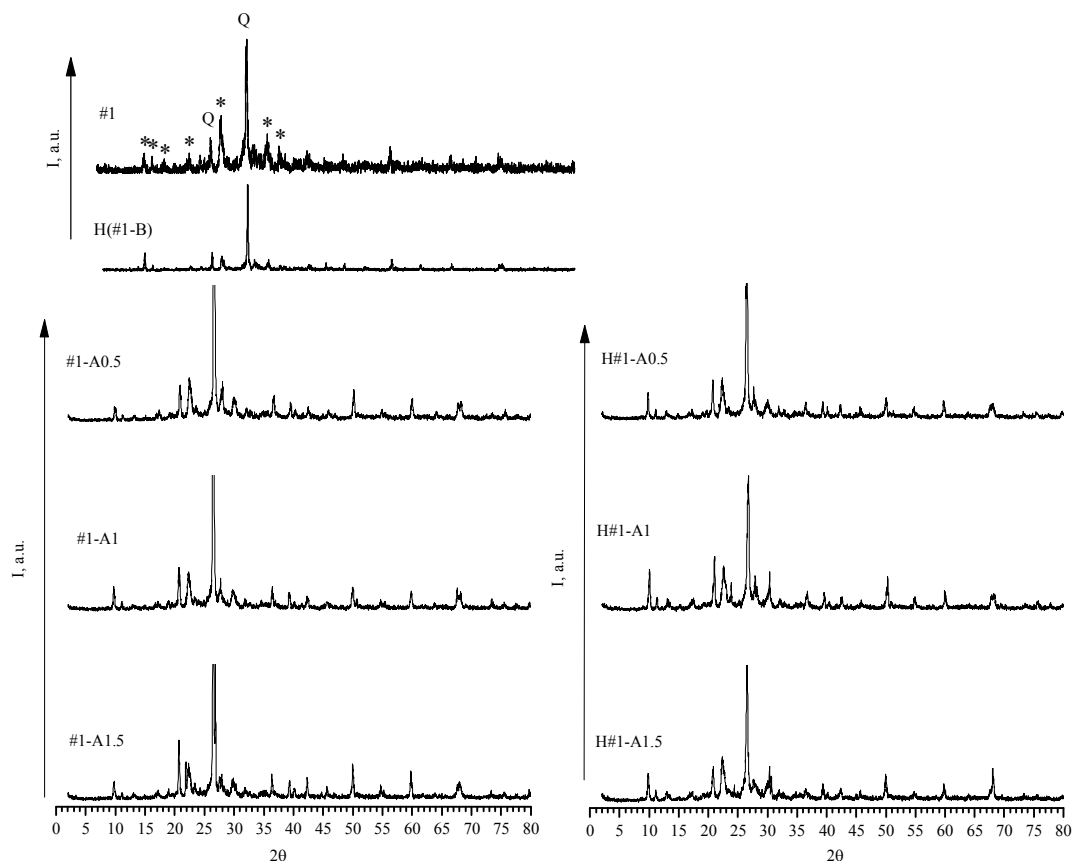


Fig. 1. X-ray diffraction patterns of the rock #1 based samples without the metal component; * – clinoptilolite, Q – the most intense reflexes of quartz

Low-temperature nitrogen ad(de)sorption was used to determine the parameters of the porous structure of the samples before adding the metal component.

The isotherm of the original rock #1 (Fig. 3) is close to the isotherm characteristic of a non-porous adsorbent, according to the IUPAC classification.²⁸ This is explained by the presence of impurity compounds in natural zeolites that narrow the channels. In the narrow channels, the diffusion of N_2 molecules can be significantly

limited by native cations. The characteristic feature of the isotherms of the modified samples is the hysteresis loop at low relative pressures up to the non-closure of the adsorption and desorption branches. This may be due to the strong adsorption of N_2 molecules near openings of narrow clinoptilolite micropores, "unblocked" as a result of the modification, which slows down their diffusion in the pores of the samples and hinders the achievement of adsorption equilibrium for the time of measurements.²⁹

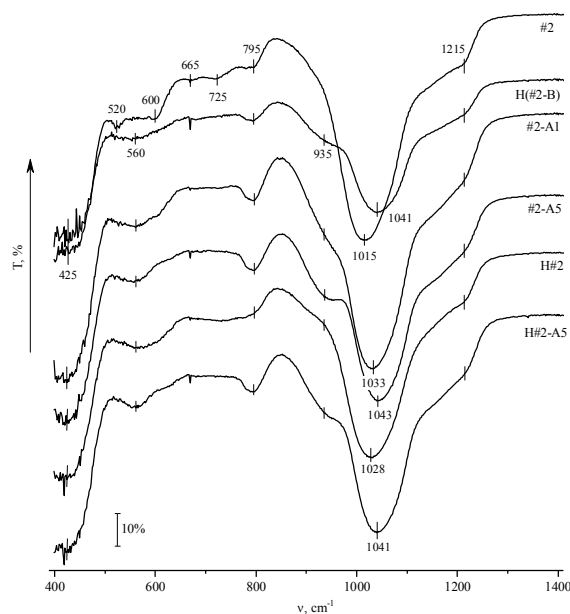


Fig. 2. IR-spectra of the modified samples of rock #2 without the metal component

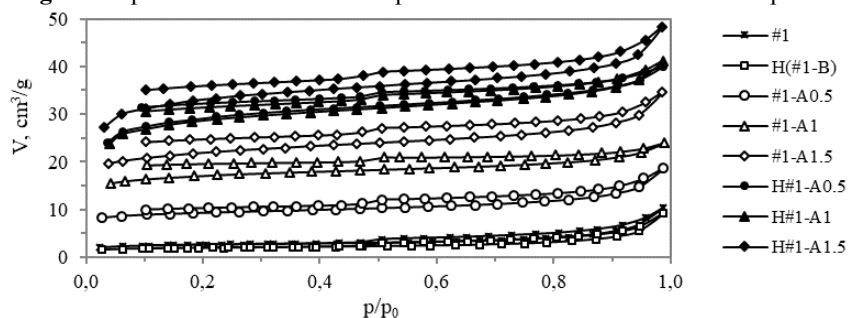


Fig. 3. Isotherms of ad(de)sorption of nitrogen ($T = 77$ K) by modified samples of rock #1 without the metal component

Table 2. Porous structure parameters of the catalysts based on rock #1

Sample	S^{BET} , m^2/g	S^t , m^2/g	S_{micro} , m^2/g	V_t , cm^3/g	V_{micro} , cm^3/g	V_{micro}/V_t , %	V_{meso} , cm^3/g	R^{DFT} , nm	R , nm
#1	9.6	3.7	5.8	0.016	0.002	13	0.014	2.64	3.3
H(#1-B)	7.1	2.8	4.3	0.014	0.002	14	0.012	2.64	4.1
#1-A0.5	35	6.3	28	0.030	0.012	41	0.018	1.17	1.7
#1-A1	64	5.4	58	0.037	0.025	67	0.012	1.25	1.2
#1-A1.5	81	8.6	72	0.053	0.032	60	0.021	1.17	1.3
H#1-A0.5	118	8.2	110	0.062	0.044	71	0.018	1.13	1.1
H#1-A1	118	9.0	109	0.064	0.043	68	0.021	1.25	1.1
H#1-A1.5	131	9.9	121	0.075	0.049	66	0.026	1.25	1.1

Note: S^{BET} is BET specific surface area; V_{micro} and S^t are micropore volume and specific surface area not counting micropores, both calculated by t -method; S_{micro} is the specific surface area of micropores, calculated as $S_{micro} = S^{BET} - S^t$; V is the total pore volume measured at $p/p_s \sim 0.99$; V_{meso} is the mesopore volume, calculated as $V_{meso} = V - V_{micro}$; R^{DFT} is the pore radius calculated by DFT; R is the average pore radius.

After modification with the alkaline solution, the porous characteristics of the sample deteriorate somewhat (Table 2). Its specific surface decreases by 25 %, and the pore volume – by 15 %. In acid-modified samples, the volume of available micropores increases significantly due to the dissolution of impurities blocking the channels. Besides, with an increase in acid concentration, all other parameters of the porous structure also tend to increase. A gradual increase in microporosity was observed along with a slight development of mesoporosity when the native rock was modified. When

using the hydrogen form as the initial form, the development of mesoporosity was not accompanied by an increase in the volume and surface of micropores, apart from the case of the most concentrated acid. This indicates that in the latter case, the micropores of the rock had already been “unblocked” by the decationation procedure. Freeing the micropores of natural zeolites from native cations seems to be essential for achieving their accessibility to adsorbate molecules. Sample H#1-A1.5 has the most developed total porosity among the catalysts based on rock #1.

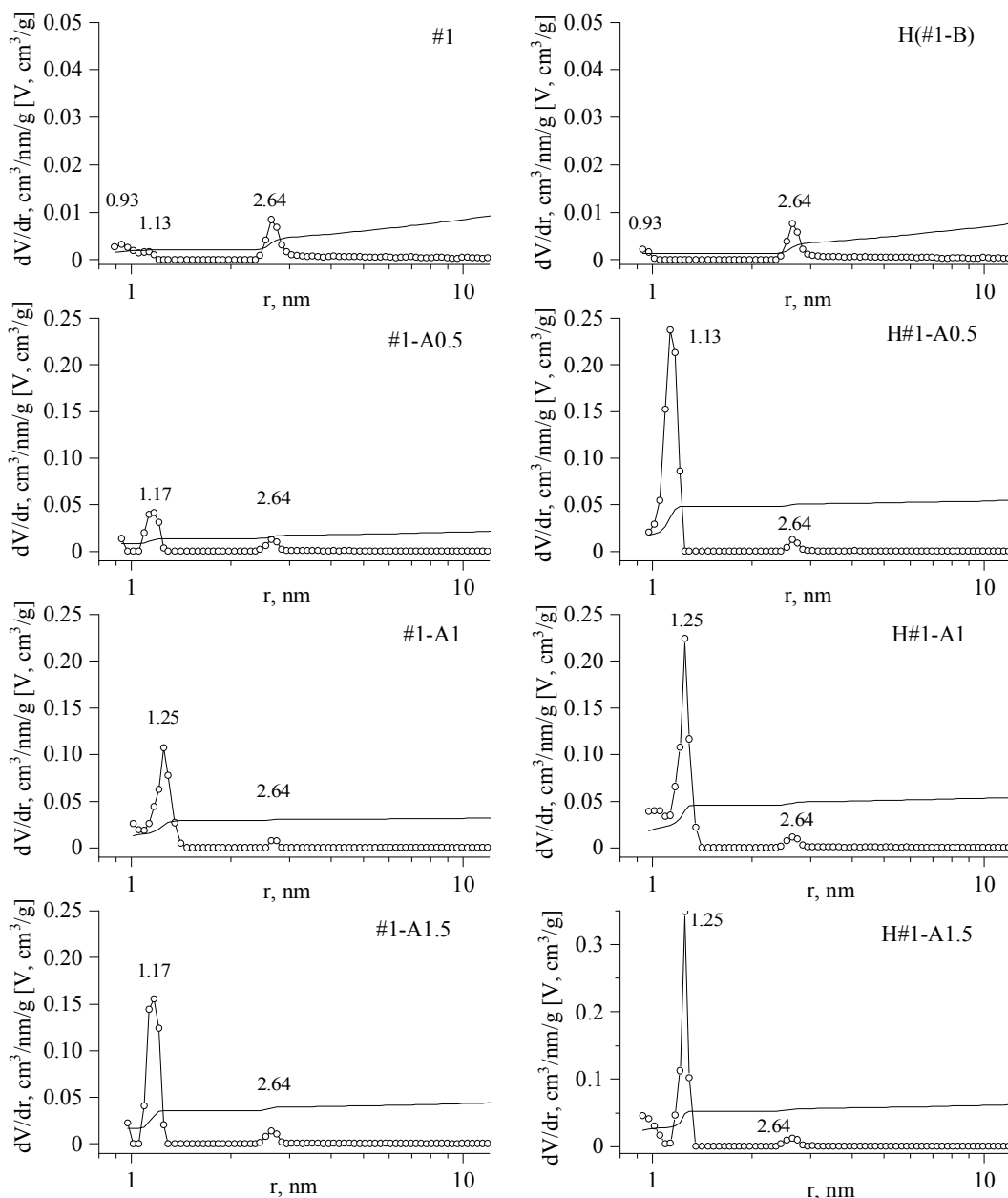


Fig. 4. DFT pore size distribution (lines with symbols) and cumulative pore volume (lines) in the samples of modified rock #1 according to the data of low-temperature N_2 ad(de)sorption

The size distribution of the mesopores of this rock has three maxima – near diameters of 2, 2.3 and 5.3 nm (Fig. 4); the first size can rather be attributed to supermicropores.²⁸ In the process of alkali modification, it does not undergo significant changes. Acid modification in the case of the native initial form contributes to the gradual increase in the volume of the narrower mesopores (~2.3 nm) when the concentration of the acid solution increases. At the same time, in all three samples obtained from the hydrogen form, the volume of such pores is

much larger, close in size, and much larger than the volume of pores with a diameter of ~5.3 nm. A higher acid concentration leads to some widening of the mesopores of smaller diameter. The effect of the modifier on these pores appears to be similar to its effect on the micropores of the rock (Table 2). The insignificant degree of development of pores with a diameter of ~5.3 nm can be explained, obviously, by the relatively low concentration of used acid solutions, which was chosen to avoid the destruction of the main, clinoptilolite, component of the rock.

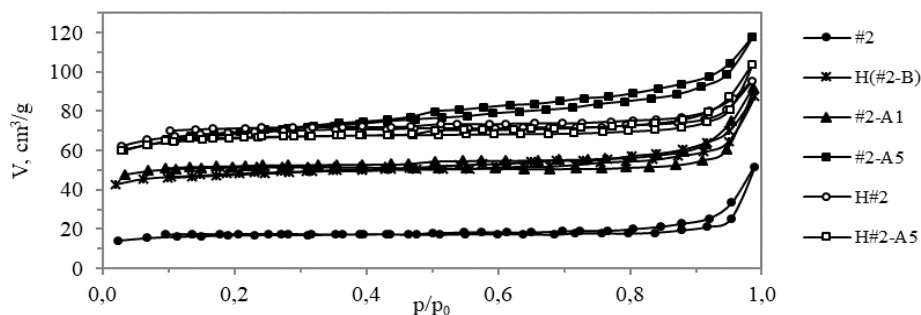


Fig. 5. Isotherms of ad(de)sorption of nitrogen ($T = 77$ K) by modified samples of rock #2 without the metal component

Table 3. Porous structure parameters of the catalysts based on rock #2

Sample	S^{BET} , m^2/g	S^t , m^2/g	S_{micro} , m^2/g	V_3 , cm^3/g	V_{micro} , cm^3/g	V_{micro}/V , %	V_{meso} , cm^3/g	R^{DFT} , nm	R , nm
#2	63	16.5	46.5	0.079	0.010	13	0.069	1.13	2.5
H(#2-B)	189	20.4	168	0.135	0.064	47	0.071	0.88	1.4
#2-A1	201	10.1	191	0.142	0.069	48	0.073	0.97	1.4
#2-A5	257	30.6	226	0.183	0.100	55	0.083	0.97	1.4
H#2	259	12.2	247	0.148	0.103	70	0.045	1.17	1.1
H#2-A5	258	10.3	247	0.160	0.097	61	0.063	1.17	1.2

The isotherm of original rock #2 in its native form is also characterized by low microporosity, however, unlike rock #1, microporosity significantly increases after modification with alkali solution as well as acid solution (Fig. 5, Table 3). Treatment with 0.2 mol/L NaOH and 1 mol/L HCl (samples H(#2-B) and #2-A1, respectively) leads to similar results, but a more successful development of the external surface is observed in the first case, while in the second one, the surface of micropores develops more successfully.

Unlike rock #1, the pore size distribution for samples based on rock #2 is characterized by only two maxima about 2 and 2.3 nm (Fig. 6); a maximum of ~5.3 nm is not observed both in the native rock and in its hydrogen form. The alkaline solution contributes to the slight development of mesopores with a wide range of sizes from 3.5 to 15 nm (samples H(#2-B)). The volume of native pores ~2 nm in this sample remains almost con-

stant, but they are slightly narrowed, which probably reflects the result of their partial blockage by the products of the rock dissolution with alkali. A solution of 1 mol/L HCl, on the contrary, develops just these pores the most.

The most noticeable increase in the volume of micropores is achieved in the decationated sample H#2 (Table 3), apparently due to the replacement of cations with protons, which confirms the assumptions made during the analysis of adsorption data for rock #1. A significant increase in the volume of micropores of rock #2 is also caused by the treatment with 5 mol/L HCl (sample #2-A5) because in this case cations are exchanged to a great extent for acid protons as well. The same concerns supermicropores, which volumes are close in samples H#2 and #2-A5 (Fig. 6). At the same time, as a result of modification of the cationic form of the rock with 5 mol/L HCl, framework aluminum is extracted, which leads, as in the case of alkali treatment, to the appearance of mesopores

3.5–15 nm in size, but somewhat larger in volume (Fig. 6). When such treatment was carried out for the hydrogen form of the rock (sample H#2-A5), the development of mesoporosity was significantly reduced due to greater acid stability of the H-form.

A similar effect of solutions of different concentrations, when a less concentrated acid mainly affected the “unblocking” of micropores, while a more concentrated acid affected the development of mesopores, was observed for acid-modified predominantly mordenite rock,¹⁴ as well as for alkali-treated mordenite catalysts.³⁰

Thus, sample #2-A5 is characterized by the largest volume of pores, both micro- and meso-, among the catalysts based on rock #2. The share of micropores in it is 55 % (Table 3), and non-uniform mesopores have a quite wide size distribution – from 2 to 10 nm. The same developed micro- and mesoporosity are characteristic of the decationated sample H#2, which was not subjected to acid/alkali modification. But this sample has a uniform system of mesopores ~2.3 nm in diameter. The share of micropores in it is 70 %.

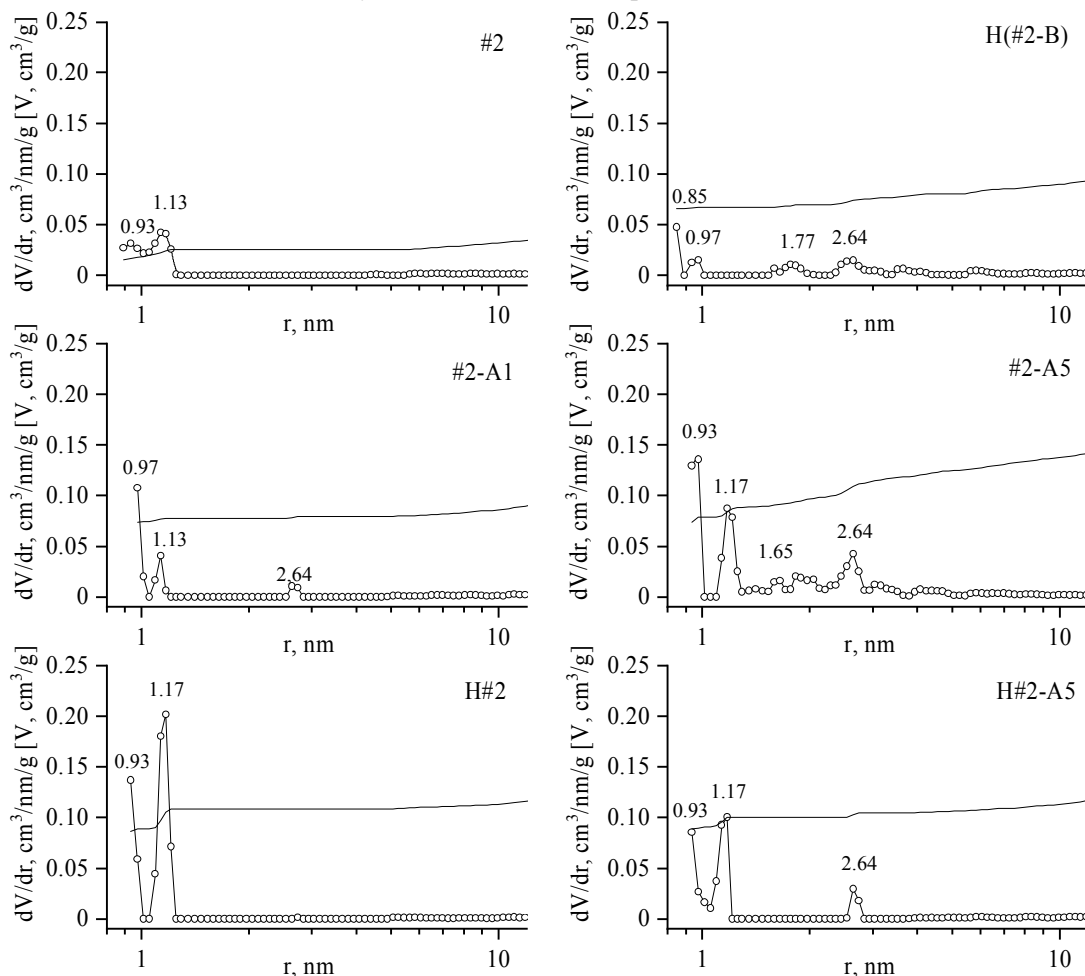


Fig. 6. DFT pore size distribution (lines with symbols) and cumulative pore volume (lines) in the samples of modified rock #2 according to the data of low-temperature N₂ ad(de)sorption

3.2. Catalytic Investigations

Catalysts based on natural zeolites were tested in the transformation of linear hexane and 2-methylpentane to evaluate their activity and determine the influence of the parameters of the porous structure on the distribution of products. Earlier,¹⁴ it was established for catalysts based on Transcarpathian zeolite rock that starting with a

content of 2.5 wt. %, nickel forms particles of a regular size of about 10 nm, which cannot be localized in narrow pores for the close interaction of acidic and hydrogenating-dehydrogenating sites. Therefore, the amount of the metal component (Ni) of 2 wt. % was chosen for application to the catalysts synthesized, which should ensure the formation of small (<10 nm) particles as close as possible to the acid sites.

The results of the catalytic tests of samples based on rock #1 are shown in Fig. 7.

First of all, it should be noted that sample #1-A1.5, both without a metal component and with an applied metal, did not show either isomerizing or cracking activity in the transformation of the hydrocarbons (Fig. 7a, b). The acid modification increased the specific surface area of the sample by almost an order of magnitude and significantly developed microporosity, but this did not have a positive effect on the catalytic efficiency of the sample. Those Brønsted acid sites,

which were formed as a result of acid treatment due to the exchange of native cations of the rock for acid protons, could not be enough to ensure its catalytic activity in these reactions, and/or the degree of “unblocking” of the active surface was insufficient.

Three catalysts based on the hydrogen form of the rock were active in the conversion of *n*-hexane as well as 2-MP (Fig. 7a, b). The main reaction products in both cases were C₁–C₅ cracking products; the yield of hexane isomers was only up to 2 % for *n*-hexane and in trace amounts for 2-MP (Fig. 7c, d).

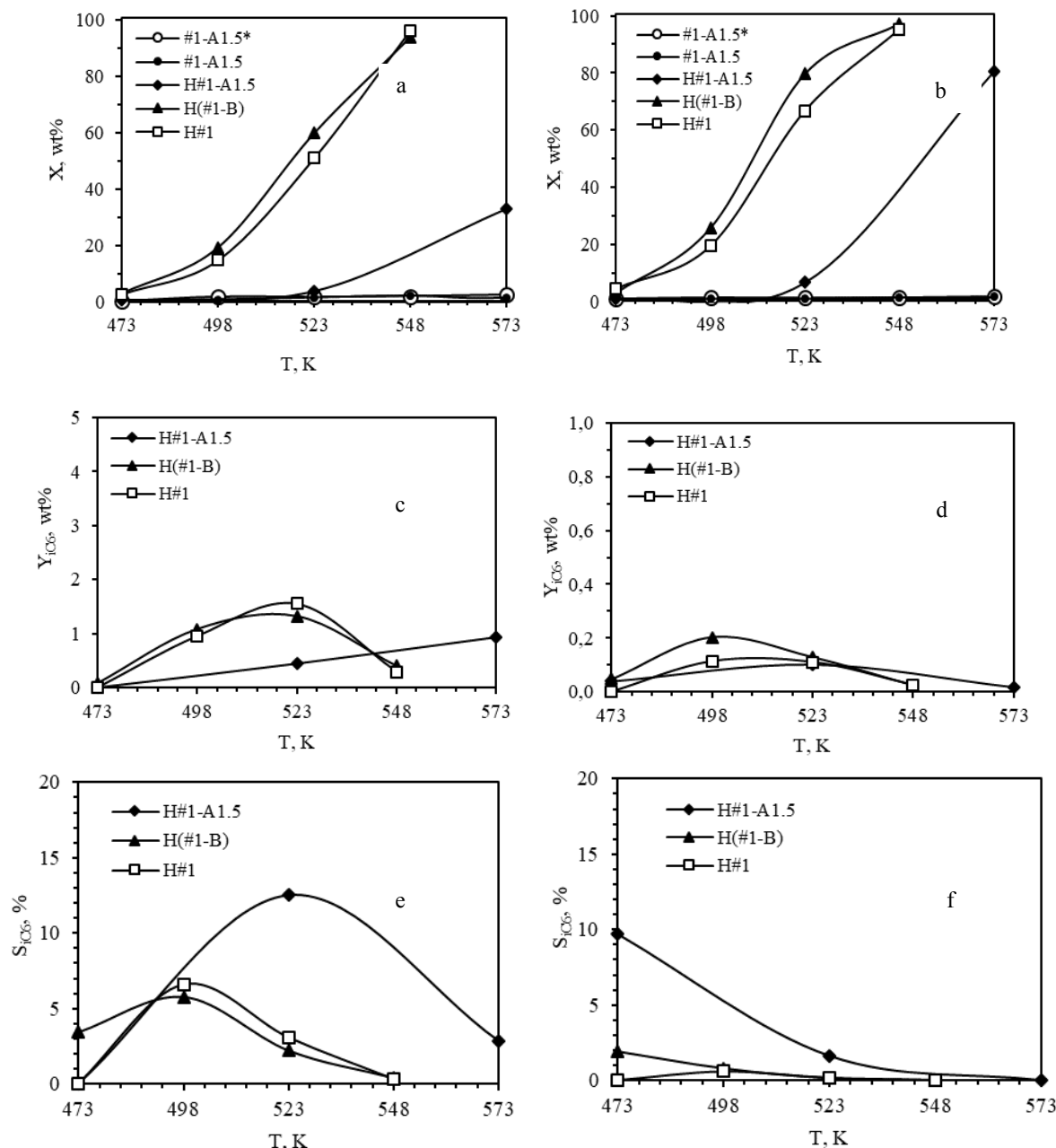


Fig. 7. Conversions X of *n*-hexane (a) and 2-MP (b), yields of hexane isomers Y_{IC6} (c, d), and isomer selectivities S_{IC6} (e, f) in the corresponding transformations on samples of modified rock #1

The catalytic properties of sample H(#1-B) are close to those of the original rock in the hydrogen form (H#1). The latter, as shown based on adsorption data in Subsection 3.1, has a developed surface of micropores, in contrast to the low porosity of the sample obtained by the alkaline treatment of rock #1 (Table 2). The similarity of the properties of these samples with significantly different porous characteristics in the transformation of both *n*-hexane and 2-MP, taking into account the sizes of their molecules (0.43 and 0.54 nm, respectively)³¹ and the effective diameter of the micropores of clinoptilolite (0.41 nm),²³ suggests that (i) the sizes of micropore openings and, of course, the micropores themselves after decationation or alkali modification did not increase compared to the sizes inherent in the clinoptilolite structure, (ii) the transformation of both hydrocarbons takes place on the surface of the open elements of the porous structure, where the concentration of the hydrogenating-dehydrogenating component of the catalyst is insignificant and the acid function prevails. These conditions and the absence of diffusion barriers contribute to a rapid and, therefore, a more complete conversion that occurs in the direction of cracking products. Isomerization has time to be realized only to a small extent on the outer surface. The micro-pulse testing mode also conduces to this.

Similarly to the original rock in H-form, sample H#1-A1.5 of acid modification is characterized by a well-developed microporosity. Despite this, the catalyst shows a noticeable decrease in the conversion of hydrocarbons compared to sample H#1, especially in the case of *n*-hexane, when it is about 30 wt. % even at 573 K (Fig. 7a, b). Simultaneously, an increase in the selectivity for hexane isomers is observed, which is more pronounced in the case of *n*-hexane (Fig. 7e, f). Obviously, the use of acid as a modifier could cause the widening of micropore openings. So, the transformation became possible on the acid sites located closer to metal particles, which have hydrogenating-dehydrogenating properties. This contributes to the increase in the selectivity for isomers. But, under such conditions, the probability of hydrogenation of carbocations formed at the initial stages of transformations increases, which, in our opinion, just leads to a decrease in conversion. The higher selectivity for *i*C₆ in the case of *n*-hexane compared to the case of 2-MP is caused by the smaller molecule size of the former and confirms the fact that the isomerization reaction occurs not on the outer surface of the zeolite rock #1.

Thus, the samples of decationated and alkali-modified rock #1, the only zeolite component of which is clinoptilolite, showed high activity in the conversion of both *n*-hexane and 2-MP into cracking products at temperatures above 498 K, but no noticeable isomerization

activity was found either for the decationated form or for the alkali- or acid-modified form.

Catalysts based on rock #2 actively convert *n*-hexane and 2-MP at temperatures above 498 and 473 K, respectively (Fig. 8a, b). The higher activity with respect to 2-MP can probably be explained by the presence of a tertiary carbon atom in its molecule, which contributes to its easier activation on Brønsted acid sites. The main reaction products, as in the case of rock #1, are C₁-C₅ cracking products (Fig. 8c,d), but the *i*C₆ yields are noticeably higher for both C₆-hydrocarbons.

The temperature dependence of the yield of *n*-hexane isomerization products has an archwire shape, demonstrating the insignificant isomerization ability of catalysts at low temperatures (Fig. 8e). The maximum yields of isomers (up to 10 wt. %) fall on 523 K for all the samples. In the case of 2-MP, isomerization begins sharply already at 473 K, and the yield of isomers at this temperature reaches 20–40 wt. % (Fig. 8f). It should be noted that 2-MP isomerizes to the same extent both to 3-MP and DMB, and to *n*-hexane. With an increase in temperature, the yields of isomers in the transformation of both hydrocarbons decrease due to increased cracking.

The original rock is the least active due to the low content of Brønsted acid sites. Alkali-modified sample H(#2-B) almost does not differ from it in all parameters.

Decationation of the native form of the rock leads to the formation of acidic OH-groups. Additionally, since rock #2 contains mordenite, the effective size of micropores of which is 0.65 nm,²³ after the "unblocking" of the pores because of decationation the inner space of the zeolite becomes easily accessible to reacting molecules of C₆-hydrocarbons. As a result, the conversion on the catalyst (sample H#2), in particular to cracking products, increases sharply (Fig. 8a-d). For the same reasons, the conversion also increases on acid-modified samples of the native form of the rock (#2-A1, #2-A5). At the same time, on these samples, along with the yield of cracking products, the yield of hexane isomers also increases – most of all at 523 K in the case of *n*-hexane conversion and at lower temperatures of 473–498 K in the case of 2-MP (Fig. 8e,f, respectively). The acid treatment of the hydrogen form (sample H#2-A5), on the contrary, leads to a decrease in the yield of cracking products of both hydrocarbons compared to initial sample H#2. Instead, the isomerization activity of the acid-treated sample H#2-A5 increases.

Obviously, the non-dealuminated H#2 catalyst contains the largest number of Brønsted acid sites. This, in particular, provides its high cracking ability, which, in turn, inhibits the competitive course of isomerization. Dealumination removes aluminum atoms associated with acid sites from the framework. The number of acid sites decreases, but they become stronger.³²

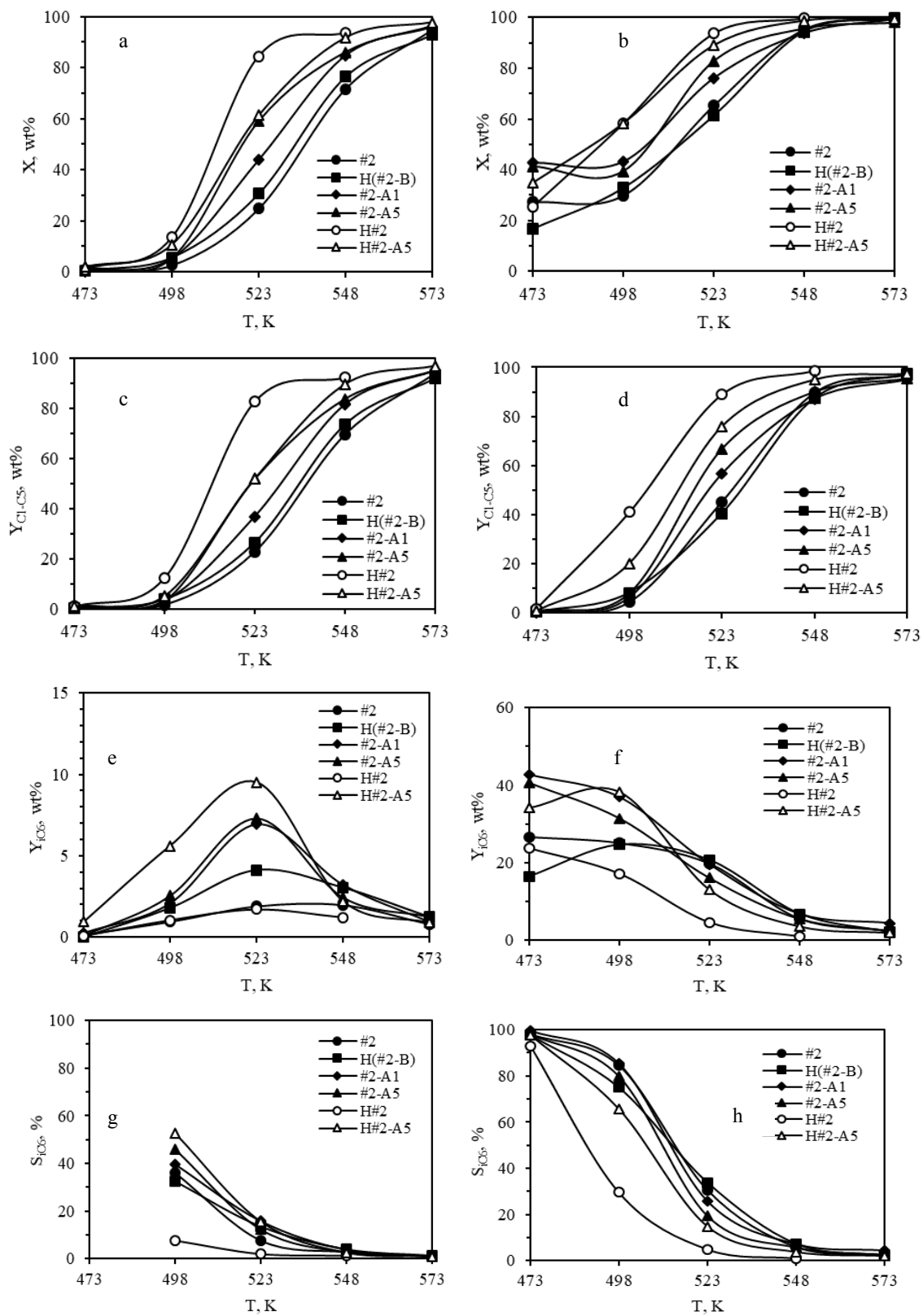


Fig. 8. Conversions X of n -hexane (a) and 2-MP (b), yields of cracking products Y_{C1-C5} (c, d) and hexane isomers Y_{iC6} (e, f), and isomer selectivities S_{iC6} (g, h) in the corresponding transformations on samples of modified rock #2

This promotes the conversion of hydrocarbons already in the direction of isomerization and weakens cracking. Since micropores of the modified samples of rock #2 is easily accessible to molecules of both *n*-hexane and 2-MP, in their conversion, the selectivity of the samples for *i*C₆ is not determined by the size of reagent molecule (Fig. 8g, h).

Thus, the most active catalyst for cracking of C₆-hydrocarbons among other catalysts based on rock #2 is a sample of decationated rock. Acid treatment inhibits cracking but promotes isomerization of both *n*-hexane and 2-MP.

4. Conclusions

The development of the porosity of clinoptilolite rock with an alkaline solution is not achieved due to the noticeable destruction of the crystalline structure of the clinoptilolite. At the same time, the alkaline treatment of clinoptilolite-mordenite rock retains its crystalline structure and causes the formation of mesopores with a wide range of sizes in the region of 3.5–15 nm; at that, the volume of native pores with a diameter of about 2 nm remains almost constant.

Modification of the rocks with hydrochloric acid solutions of low concentration (up to 1–1.5 mol/L), and especially their decationation, leads to an increase in the volume of micropores and narrow native mesopores with a diameter near 2 nm. The effect of more concentrated solutions, in addition, is the development of irregular mesoporosity in the size range from 3.5 to 15 nm. In the case of more acid-resistant hydrogen form, the development of such mesopores is significantly reduced.

Catalysts based on decationated and alkali-modified clinoptilolite rocks demonstrate high activity in the cracking reaction of *n*-hexane and 2-methylpentane at 523–548 K. The transformation of both linear and branched hydrocarbons occurs on the surface of the open elements of the porous structure of the samples. Since there is no need for deep decationation of the rock, this can simplify a catalyst preparation procedure. Also, the inaccessibility of the micropores of the catalyst leads to a shorter contact time of reaction products with active sites, which prevents over-cracking of them.

In the case of clinoptilolite-mordenite rock, transformations occur in the inner space of the pores too. Having a larger number of accessible acid sites, more developed microporosity, and a system of narrow mesopores, the decationated sample of this rock is a more active catalyst of cracking compared to a similar catalyst based on a clinoptilolite rock. Acid modification of clinoptilolite-mordenite rock promotes isomerization of both studied C₆-hydrocarbons.

Thus, results of the work show that decationation and/or modification with hydrochloric acid makes it pos-

sible to obtain active catalysts of the conversion of C₆-hydrocarbons based on clinoptilolite-containing rocks of Transcarpathia of different phase composition. The development of microporosity and a system of narrow mesopores with a diameter of about 2 nm plays an important role in improving the performance of rocks in the conversion of C₆-hydrocarbons, in contrast to the presence of wider mesopores of 3.5–15 nm in a size.

Acknowledgments

The authors express their gratitude to Candidate of physical and mathematical sciences M.M. Filonenko, the deputy head of the department for career guidance work, associate professor at University of the State Fiscal Service of Ukraine, for assistance in obtaining the diffraction patterns of the samples.

References

- [1] Patrylak, L.; Pertko, O. Peculiarities of Activity Renovation of Zeolite Catalysts Coked in Hexane Cracking. *Chem. Chem. Technol.* **2018**, *12*, 538–542. <https://doi.org/10.23939/chcht12.04.538>
- [2] Barakov, R.Y.; Shcherban, N.D.; Yaremov, P.S.; Voloshyna, Y.G.; Krylova, M.M.; Tsyryna, V.V.; Ilyin, V.G. Effect of the Structure and Acidity of Micro-Mesoporous Aluminosilicates on Their Catalytic Activity in Cumene Cracking. *Theor. Exp. Chem.* **2016**, *52*, 212–220. <https://doi.org/10.1007/s11237-016-9470-x>
- [3] Liu, Z.; Hua, Y.; Wang, J.; Dong, X.; Tian, Q.; Han, Y. Recent Progress in the Direct Synthesis of Hierarchical Zeolites: Synthetic Strategies and Characterization Methods. *Mater. Chem. Front.* **2017**, *1*, 2195–2212. <https://doi.org/10.1039/C7QM00168A>
- [4] Kurmach, M.M.; Larina, O.V.; Kyriienko, P.I.; Yaremov, P.S.; Trachevsky, V.V.; Shvets, O.V.; Soloviev, S.O. Hierarchical Zr-MTW Zeolites Doped with Copper as Catalysts of Ethanol Conversion into 1,3-Butadiene. *ChemistrySelect.* **2018**, *3*, 8539–8546. <https://doi.org/10.1002/slct.201801971>
- [5] Bai, R.; Song, Y.; Li, Y.; Yu, J. Creating Hierarchical Pores in Zeolite Catalysts. *Trends in Chemistry* **2019**, *1*, 601–611. <https://doi.org/10.1016/j.trechm.2019.05.010>
- [6] Khan, W.; Jia, X.; Wu, Zh.; Choi, J.; Yip, A.C.K. Incorporating Hierarchy into Conventional Zeolites for Catalytic Biomass Conversions: A Review. *Catalysts* **2019**, *9*, 127–150. <https://doi.org/10.3390/catal9020127>
- [7] Martins, G.S.V.; dos Santos, E.R.F.; Rodrigues, M.G.F.; Pecchi, G.; Yoshioka, C.M.N.; Cardoso, D. N-Hexane Isomerization on Ni-Pt/Catalysts Supported on Mordenite. *Modern Research in Catalysis* **2013**, *2*, 119–126. <https://doi.org/10.4236/mrc.2013.24017>
- [8] Sousa, B.V.; Brito, K.D.; Alves, J.J.N.; Rodrigues, M.G.F.; Yoshioka, C.M.N.; Cardoso, D. N-Hexane Isomerization on Pt/HMOR: Effect of Platinum Content. *React. Kinet. Mech. Cat.* **2011**, *102*, 473–485. <https://doi.org/10.1007/s11144-010-0273-0>
- [9] Ono, Y. A Survey of the Mechanism in Catalytic Isomerization of Alkanes. *Catal. Today* **2003**, *81*, 3–16. [https://doi.org/10.1016/S0920-5861\(03\)00097-X](https://doi.org/10.1016/S0920-5861(03)00097-X)
- [10] Patrljak, K.I.; Bobonich, F.M.; Patrljak, L.K.; Voloshina, Yu.G.; Levchuk, N.N.; Solomaha, V.N.; Cuprik, I.N. Gidroizomerizacija N-Geksana na Palladij- i Cirkonilsoderzhashhih Modificirovannyh Mordenit-Klinoptilolitovyh Porodah. *Kataliz ta naftohimiã* **2000**, *4*, 10–15.

- [11] Patrylak, K.I.; Bobonich, F.M.; Tsupryk, I.N.; Bobik, V.V.; Levchuk, N.N.; Solomakha, V.N. The Role of External Acid Sites of Palladium-Containing Zeolite Catalysts in Hexane Isomerization. *Pet. Chem.* **2003**, *43*, 387–394.
- [12] Bobik, V.V.; Bobonich, F.M.; Belokopytov, Yu. V. Effect of External Acidity of Mordenite-Supported Catalysts on the 2,2-Dimethylbutane Content in Hydroisomerization Products of N-Hexane. *Theor. Exp. Chem.* **2003**, *39*, 364–368. <https://doi.org/10.1023/B:THEC.0000013989.04033.e1>
- [13] Patrylak, L.K.; Pertko, O.P.; Yakovenko, A.V.; Voloshyna, Yu.G.; Povazhnyi, V.A.; Kurmach, M.M. Isomerization of Linear Hexane over Acid-Modified Nanosized Nickel-Containing Natural Ukrainian Zeolites. *Appl. Nanosci.* **2022**, *12*, 411–425. <https://doi.org/10.1007/s13204-021-01682-1>
- [14] Voloshyna, Yu.G.; Pertko, O.P.; Povazhnyi, V.A.; Patrylak, L.K.; Yakovenko, A.V. Influence of the Development of a System of Nanoscale Pores in a Mordenite-Containing Rock on Its Selectivity for Di-Branched Products of n-Hexane Hydroisomerization. *Appl. Nanosci.* [Online early access]. <https://doi.org/10.1007/s13204-022-02632-1> Published online: September 13, 2022. <https://www.springer.com/journal/13204> (accessed Oct 15, 2022).
- [15] Woo, H.C.; Lee, K.H.; Lee, J.S. Catalytic Skeletal Isomerization of N-Butenes to Isobutene over Natural Clinoptilolite Zeolite. *Appl. Catal. A-Gen.* **1996**, *134*, 147–158. [https://doi.org/10.1016/0926-860X\(95\)00216-2](https://doi.org/10.1016/0926-860X(95)00216-2)
- [16] Dziejzicka, A.; Sulikowski, B.; Ruggiero-Mikolajczyk, M. Catalytic and Physicochemical Properties of Modified Natural Clinoptilolite. *Catal. Today* **2016**, *259*, 50–58. <https://doi.org/10.1016/j.cattod.2015.04.039>
- [17] Miądlicki, P.; Wróblewska, A.; Kielbasa, K.; Koren, Z.C.; Michalkiewicz, B. Sulfuric Acid Modified Clinoptilolite as a Solid Green Catalyst for Solvent-Free α -Pinene Isomerization Process. *Microporous Mesoporous Mater.* **2021**, *324*, 111266. <https://doi.org/10.1016/j.micromeso.2021.111266>
- [18] Retajczyk, M.; Wróblewska, A.; Szymańska, A.; Michalkiewicz, B. Isomerization of Limonene over Natural Zeolite-Clinoptilolite. *Clay Minerals* **2019**, *54*, 121–129. <https://doi.org/10.1180/clm.2019.18>
- [19] Khoshbin, R.; Haghighi, M.; Asgari, N. Direct Synthesis of Dimethyl Ether on the Admixed Nanocatalysts of CuO–ZnO–Al₂O₃ and HNO₃-Modified Clinoptilolite at High Pressures: Surface Properties and Catalytic Performance. *Mater. Res. Bull.* **2013**, *48*, 767–777. <https://doi.org/10.1016/j.materresbull.2012.11.057>
- [20] Yilmaz, S.; Ucar, S.; Artok, L.; Gulec, H. The Kinetics of Citral Hydrogenation over Pd Supported on Clinoptilolite Rich Natural Zeolite. *Appl. Catal. A-Gen.* **2005**, *287*, 261–266. <https://doi.org/10.1016/j.apcata.2005.04.002>
- [21] Barthomeuf, D. Zeolite Acidity Dependence on Structure and Chemical Environment. Correlations with Catalysis. *Mater. Chem. Phys.* **1987**, *17*, 49–71. [https://doi.org/10.1016/0254-0584\(87\)90048-4](https://doi.org/10.1016/0254-0584(87)90048-4)
- [22] Tur'yan, Y.I. Theoretical Bases of the Ammonium Ion Determination by Formol Titration. *Rev. Anal. Chem.* **2010**, *29*, 25–37. <https://doi.org/10.1515/REVAC.2010.29.1.25>
- [23] Database of Zeolite Structures Home Page. <http://www.iza-structure.org/databases/> (accessed 2022-10-15).
- [24] Zuo, R.-F.; Du, G.-X.; Yang, W.-G.; Liao, L.-B.; Li, Z. Mineralogical and Chemical Characteristics of a Powder and Purified Quartz from Yunnan Province. *Open Geosci.* **2016**, *8*, 606–611. <https://doi.org/10.1515/geo-2016-0055>
- [25] Pechar, F.; Rykl, D. Study of the Complex Vibrational Spectra of Natural Zeolite Mordenites. *Zeolites* **1983**, *3*, 329–332. [https://doi.org/10.1016/0144-2449\(83\)90177-X](https://doi.org/10.1016/0144-2449(83)90177-X)
- [26] Jansen, J.C.; van der Gaag, F.J.; van Bekkum, H. Identification of ZSM-type and Other 5-Ring Containing Zeolites by I.R. Spectroscopy. *Zeolites* **1984**, *4*, 369–372. [https://doi.org/10.1016/0144-2449\(84\)90013-7](https://doi.org/10.1016/0144-2449(84)90013-7)
- [27] Patrylak, L.K.; Voloshyna, Yu.G.; Pertko, O.P.; Yakovenko, A.V.; Povazhnyi, V.A.; Melnychuk, O.V. Investigation of the Features of Nickel-Modified Mordenite Zeolites. *Water&Water Purification Technologies. Scientific and Technical News* **2021**, *30*, 59–66. <https://doi.org/10.20535/2218-930022021241332>
- [28] Thommes, M.; Kaneko, K.; Neimark, A.V.; Olivier, J.P.; Rodriguez-Reinoso, F.; Rouquerol, J.; Sing, K.S.W. Physisorption of Gases, With Special Reference to the Evaluation of Surface Area and Pore Size Distribution (IUPAC Technical Report). *Pure Appl. Chem.* **2015**, *87*, 1051–1069. <https://doi.org/10.1515/pac-2014-1117>
- [29] Hernández, M.; Rojas, F.; Lara, V. Nitrogen-Sorption Characterization of the Microporous Structure of Clinoptilolite-Type Zeolites. *J. Porous Mater.* **2000**, *7*, 443–454. <https://doi.org/10.1023/A:1009662408173>
- [30] Monteiro, R.; Ani, C.O.; Rocha, J.; Carvalho, A.P.; Martins, A. Catalytic Behavior of Alkali-Treated Pt/HMOR in N-Hexane Hydroisomerization. *Appl. Catal. A-Gen.* **2014**, *476*, 148–157. <https://doi.org/10.1016/j.apcata.2014.02.026>
- [31] Gobin, O.C.; Reitmeier, S.J.; Jentys, A.; Lercher, J.A. Role of the Surface Modification on the Transport of Hexane Isomers in ZSM-5. *J. Phys. Chem. C* **2011**, *115*, 1171–1179. <https://doi.org/10.1021/jp106474x>
- [32] Barthomeuf, D. Topology and Maximum Content of Isolated Species (Al, Ga, Fe, B, Si, ...) in a Zeolitic Framework. An Approach to Acid Catalysis. *J. Phys. Chem.* **1993**, *97*, 10092–10096. <https://doi.org/10.1021/j100141a032>

Received: October 15, 2022 / Revised: December 24, 2022 / Accepted: January 02, 2023

ВПЛИВ МОДИФІКУВАННЯ КЛИНОПТИЛОЛІТВИСНИХ ПОРІД ЗАКАРПАТТЯ НА ЇХНІ ПОРИСТІ ХАРАКТЕРИСТИКИ І КАТАЛІТИЧНІ ВЛАСТИВОСТІ В ПЕРЕТВОРЕННІ C₆-ВУГЛЕВОДНІВ

Анотація. На основі даних рентгенівської дифрактометрії, ІЧ-спектроскопії, низькотемпературної адсорбції N₂ та тестування в мікроімпульсному каталітичному перетворенні C₆-вуглеводнів було оцінено ефективність модифікування українських клиноптилолітвісних порід, здійсненого з метою покращення їхніх адсорбційних і каталітичних властивостей. Встановлено вплив такого модифікування на розподіл продуктів реакції.

Ключові слова: цеолітвісна порода, біфункціональний каталізатор, модифікування, C₆-вуглеводні, крекінг, гідроізомеризація.